Available online at www.sciencedirect.com
ScienceDirect
International Journal of Mass Spectrometry 267 (2007) 190–198
International Journal of Mass Spectrometry
www.elsevier.com/locate/ijms

A new technique for studying ion–ion recombination in a flowing afterglow Langmuir probe apparatus: Ar^+ recombining with Cl_2^-, CCl_2O^-, Br_2^-, SF_5^- and SF_6^-

Thomas M. Miller [a], Jeffrey F. Friedman [b], A.A. Viggiano [a,*]

[a] *Air Force Research Laboratory, Space Vehicles Directorate, Hanscom Air Force Base, Bedford, Massachusetts 01731-3010, USA*
[b] *Department of Physics, University of Puerto Rico, Mayaguez, Puerto Rico 00681-9016, USA*

Received 16 November 2006; received in revised form 29 January 2007; accepted 20 February 2007
Available online 24 February 2007

Abstract

We present a new technique for measuring ion–ion recombination rate constants in a flowing afterglow Langmuir probe (FALP) apparatus. The technique involves measuring the fractional negative ion product distribution following electron attachment versus the initial electron density when two or more products are formed. The concentration of reactant gas is kept low enough that the plasma retains its electron-Ar^+, ambipolar diffusion character along the entire length of the flow tube. If only polyatomic anions are formed, accurate relative rates are obtained. When one of the species is atomic, absolute rates are also possible by doing a detailed model of the plasma kinetics. Here we present rate constants for Ar^+ recombining with Cl_2^- ($(5.3 \pm 1.6) \times 10^{-8}$ cm^3 s^{-1} at 302 K), Br_2^- ($(3.9 \pm 1.2) \times 10^{-8}$ cm^3 s^{-1} at 302 K), the phosgene negative ion CCl_2O^- ($(8.9 \pm 2.7) \times 10^{-8}$ cm^3 s^{-1} at 302 K), and relative rate constants for $Ar^+ + SF_6^-$ and SF_5^- (ratio 1.2 at 550 K, with an uncertainty of +0.3 and −0.1). The diatomic negative ions are found to recombine slower than the polyatomic ones, in agreement with earlier indications.

Keywords: Ion–ion recombination; Ion–ion mutual neutralization; Flowing afterglow Langmuir probe; FALP; Ar^+; Cl_2^-; Br_2^-; CCl_2O^-; SF_6^-; SF_5^-

1. Introduction

Elementary reactions in plasmas include electron attachment to neutral molecules, ion–neutral reactions of various types, electron–positive ion recombination, and positive ion–negative ion recombination (more properly, mutual neutralization) [1]. The first three classes of reaction have been well studied. Many techniques have been used to study electron attachment under a variety of conditions and numerous reviews have been published [2–5]. Electron attachment is critical to the present work, as shown below. Ion–neutral reactivity is the best studied class of plasma reactions and thousands of such systems have been examined. A recent compilation by Anicich consists of over 1000 pages of positive ion reactions alone [6]. While no recent compilation exists for negative ion–neutral systems, they are also well studied [7]. Historically, both electron–ion and ion–ion recombination reactions have been the most difficult to study, since one must generate plasmas (or crossed beams) of sufficient intensity and purity to make accurate measurements on well defined systems [8]. For electron–positive ion recombination the advance of storage ion rings has changed the situation and many reactions have now been studied [9,10]. In contrast, the study of positive ion–negative ion recombination has seen little progress in many years [11].

Because of the strong, long-range Coulomb potential between the interacting positive and negative ions, ion–ion recombination is characterized by large cross sections, as much as 10,000 Å^2, at low energies. In most cases, the reaction is highly exothermic, so the products may be electronically excited or even dissociated [12,13].

Recognition of the ion–ion recombination process dates back to work of J.J. Thomson and Ernest Rutherford in 1896, according to the history given by Loeb [14]. Thomson and Rutherford showed that the decay in the ion density of an afterglow plasma depended on the product of the positive and negative ion densities, with a proportionality denoted by α, the recombination

* Corresponding author.
E-mail address: albert.viggiano@hanscom.af.mil (A.A. Viggiano).

1387-3806/$ – see front matter © 2007 Elsevier B.V. All rights reserved.
doi:10.1016/j.ijms.2007.02.033

rate constant. Many subsequent experimental studies of ion–ion recombination were conducted out over the past century in pulsed afterglows or flames. As far back as 1938, laboratory data on ion–ion recombination in air were compared with atmospheric conductivity measurements carried out on tropospheric and stratospheric balloons flights, as it was recognized that ion–ion recombination was the process which limited the ion density in the atmosphere [15]. While these works generally mapped out the behavior of α with pressure, which varied from a binary interaction at low pressure through a peak around 1 atm to a mobility-limited decrease at higher pressures, the identity of the ions (which could change with pressure) was never certain. The first mass spectrometric work seems to be that of Greaves in 1964 [16] and of Fisk et al. in 1967 [17]. Fisk et al. determined recombination rate constants ($(6–14) \times 10^{-8}$ cm^3 s^{-1}) for various mixtures of ions formed from Tl halides and Pb iodide in 10–54 kPa of Ar buffer gas from 530–707 K. More direct measurements were made by Hirsch et al. around 1970, in which values of α of 5×10^{-8} ($NO^+ + NO_3^- \rightarrow$ neutrals) and 2×10^{-7} cm^3 s^{-1} ($NO^+ + NO_2^- \rightarrow$ neutrals) were measured at 300 K in 0.3–3 kPa of air-like N_2–O_2 mixtures [18]. At about the same time, a merged beams apparatus came online at SRI International, in which the merging magnet also provided the mass selection, in connection with Wien filters [13]. The apparatus was used to measure many atomic and molecular ion–ion recombination cross sections, from 0.15–200 eV. Rate constants (from $(1–8) \times 10^{-7}$ cm^3 s^{-1}) were deduced for use in atmospheric modeling, with the caveat that the fast beams might consist of vibrationally excited ions, or even contain metastable electronically-excited ions [12]. Shortly afterwards, around 1976, the flowing-afterglow Langmuir-probe technique (FALP) was developed at the University of Birmingham (UK) to study electron attachment, electron–ion recombination, and ion–ion recombination in a thermally-equilibrated He buffer gas, with mass analysis of the ions [19]. Ion–ion recombination rate constants obtained with this experiment [20], in the range $(4.0–9.6) \times 10^{-8}$ cm^3 s^{-1}, were quite a bit lower than measured in the SRI work, implying that the decay of ionization in the upper atmosphere would be much slower than previously thought.

In connection with the SRI experiments, Olson developed theory for ion–ion recombination based on Landau–Zener curve crossings between the incoming Coulomb potential and the outgoing neutral curves, which are essentially flat in the crossing region [21]. Because of problems inherent in Landau–Zener theory and approximations for the coupling matrix element in the region of the curve crossings, the theoretical cross sections are considered accurate only at the factor-of-2-or-3 level [13,21]. Recombination between atomic ions may involve a few or a dozen favorable crossings. For molecular ions, the number of crossings may be in the hundreds because of the number of excited electronic and vibrational states crossing the Coulomb curve. For such cases, Olson developed an "absorbing sphere" model, with unit capture within a critical radius derived from Landau–Zener theory [22]. Based on results from Olson's absorbing sphere theory, Hickman [23] developed a parameterized formula for α, which is given here as modified to fit the FALP data [24]:

$$\alpha = 5.33 \times 10^{-7}\,\mathrm{cm^3\,s^{-1}} (300/T)^{0.50}\,\mathrm{m^{-0.52}}\,E_{be}^{-0.24}, \quad (1)$$

where T is in K, m is the ion pair reduced mass in atomic mass units, and E_{be} is the electron binding energy of the negative ion, in eV. This semiempirical formula fits much of the 300 K data to within ±30%, but the formula has only been minimally tested. For example, most negative ions studied with the FALP apparatus have moderately large E_{be}, the one exception being that of SF_6^-, at 1.05 eV [25]. The present work, with the phosgene negative ion (E_{be} = 1.17 eV [26]), adds one datum for negative ions of low E_{be} (among ions studied with the FALP). Still, for the ions studied in the present work, Eq. (1) only predicts a variation in recombination rate constants from $6–9 \times 10^{-8}$ cm^3 s^{-1} at 300 K. (Even a fixed value of 6.75×10^{-8} cm^3 s^{-1} would fit the FALP data within ±42%.) Thus, a stringent test of Eq. (1), leading either to improved exponents or failure of the formula, requires more accurate data, and remains for future work.

Recombination between two atomic ions is a special case because few curve crossings may occur [13,27]. The few avoided curve crossings allowed Olson to apply quantum close coupling theory to obtain rate constants for $Na^+ + Cl^-$ (3.7×10^{-9} cm^3 s^{-1}) and $K^+ + Cl^-$ (8.5×10^{-11} cm^3 s^{-1}) at 300 K [27]. Church and Smith made a heroic effort to measure recombination rates for rare-gas positive ions with Cl^- and F^-, in a FALP apparatus, but could only establish upper limits of typically 5×10^{-9} cm^3 s^{-1} [28]. That is, in their cases, any recombination loss was indistinguishable from diffusive losses. In none of those cases would Eq. (1), based on the absorbing sphere model [22], be applicable. Even for a diatomic negative ion recombining with Ar^+, e.g. Cl_2^-, there may only be one favorable curve crossing [29].

Ion–ion recombination has also been studied in inclined beam experiments [30,31]. While such experiments cannot approach the thermal region of interaction energy of relevance here, they have produced intriguing results, notably for $He^+ + H^- \rightarrow He + H$, where oscillations were seen in the cross section versus energy, and good agreement with theory for the average values was found [31]. Ion–ion recombination has also been studied in atmospheric-pressure flames (see [32], for example, with mass spectrometric results obtained at 2582 K), and the reverse process, chemiionization, has also been studied [33].

The FALP apparatus has been used to study electron and ion reactions with neutrals, and electron–ion and ion–ion recombination, perhaps the only instrument capable of such versatility, aside from the generality of crossed or merged beams apparatuses [5,11,20,34,35]. In this article we report a new approach in the use of the FALP for studies of positive ion–negative ion recombination. The technique relies both on the mass spectrometer and the Langmuir probe. It requires detailed modeling of the plasma to derive absolute rate constants which in part limits the accuracy to ±30%. However, relative rate constants should be measured quite accurately, i.e. to approximately ±10% percent or possibly better. Here, we present the initial studies involving rate constants for Ar^+ recombination with Br_2^-, Cl_2^-, CCl_2O^-,

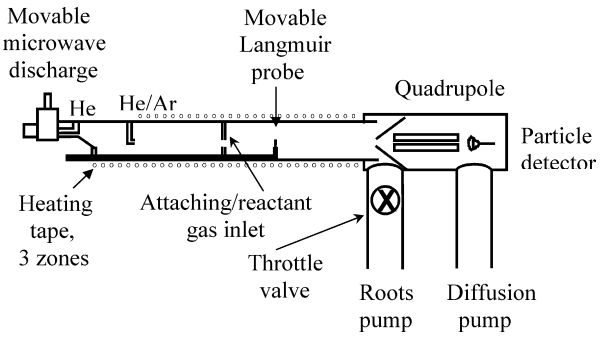

Fig. 1. A sketch of the FALP apparatus. The gas flow is from left to right. The flow tube has 3.65 cm inside radius, and is about 1 m in length.

SF_5^- and SF_6^-, and discuss the advantages and limitations of the method.

2. Experimental

The FALP apparatus used at the Air Force Research Laboratory (AFRL) is shown schematically in Fig. 1 [35,36]. Electrons, He^+, and He^* (metastable-excited He) were created in a microwave discharge in a fast flow of He buffer gas in the FALP. A few percent Ar gas was added downstream of the source, to convert He^* and He_2^+ into Ar^+ such that the positive ion mass spectrum showed approximately 98% Ar^+, 1% other atomic positive ions, and 1% molecular positive ions.[1] The negative charge approached 100% electrons. While these analyses were determined using a downstream mass spectrometer, i.e. after ~8 ms reaction time, enough Ar was added to ensure that the chemistry was complete shortly after the Ar port and well before the introduction of the reactant gas. The small impurity levels were accounted for in the data analysis and turned out to have little effect on the results.

Electron concentrations were determined with a Langmuir probe that has been described in detail previously [35,37]. Briefly, current was measured as a function of applied voltage to a small tungsten wire (25 μm diameter, 40 mm long) at the axis of the flow tube. The Mott-Smith and Langmuir equation [38] was then used to derive the electron density, as described in detail for the FALP apparatus by Španěl [37]. Absolute electron densities are required for measurements of ion–ion recombination. The primary uncertainty (estimated at 10%) in the absolute electron densities comes from knowing the effective length of the probe, because of the distortion of the plasma sheath by the larger-diameter glass support tube. Relative electron densities are thought to be precise to 3%. A second uncertainty concerns the applicability of the Mott-Smith and Langmuir equation only to collisionless collection of charge from the plasma sheath. Several tests of this requirement have been carried out, for rare gas buffers in the pressure range used with the FALP, with the result that electron densities are accurately measured, but that ion densities will be overestimated, depending on the plasma density, by a factor of up to 1.2 for our 133 Pa of He buffer gas [39–42]. For high plasma densities ($\approx 10^{10}$ cm^{-3}), the sheath radius around the probe is small enough that negligible error occurs [41]. For low plasma densities ($\approx 10^{7}$ cm^{-3}), the apparent (erroneous) ion density will be several times the (correct) electron density [41]. We emphasize that the Langmuir probe is operating as designed, collecting currents from the plasma; the issue is interpretation of the collected currents in terms of electron and ion densities in the plasma, that is, whether the orbital motion limited theory, or continuum theory, or something in between, is the appropriate model for obtaining the ion density. This uncertainty in using the Langmuir probe to measure ion densities is one of the motivations for the present work, which relies on the Langmuir probe only for determining the initial electron density. That is, the Langmuir probe remains fixed near the port where reactant gas enters the flow tube through four radially-oriented glass capillaries. The present approach opens the possibility of measuring ion–ion recombination rate constants for He pressures from 70 to perhaps 700 Pa. As noted by Johnsen et al. [40], one can check on the validity of the Langmuir probe data at different He pressures by the measuring rate constant for electron–O_2^+ recombination, which is known to be independent of pressure, at least for low pressures of rare gases [43,44]. Discussion of the pressure dependence of ion–ion recombination rate constants is beyond the scope of the present article; the reader is referred to [44]. Preliminary data on ion–ion recombination rate constants measured up to 1.1 kPa He pressure were given in [20], but subsequent work on the problems of deducing ion concentrations using a cylindrical Langmuir probe [40] suggest that the pressure dependence is not nearly as strong as reported.

Accordingly, the Langmuir probe used in the present work was checked by measuring the rate constant for electron–O_2^+ recombination, for which there is general agreement for a value close to 2.0×10^{-7} cm^3 s^{-1} at 300 K [43,45]. For this test, we measured the electron concentration, n_e, along the flow tube axis over a reaction time of 2 ms (20 cm along the flow tube axis) and plotted $1/n_e$ versus reaction time [43,45], yielding slopes of 2.1 (three data sets) and 2.2 (one data set) $\times 10^{-7}$ cm^3 s^{-1}. These results imply that the n_e values measured with the probe are accurate within about 10%.

Without an attaching gas, plasma is lost by ambipolar diffusion, since the atomic ion, Ar^+, does not recombine with electrons, except in three-body collisions. The diffusion frequency is determined by measuring the exponential decay in electron concentration along the flow tube axis, in absence of reactant. In the present work on ion–ion recombination, the electron-attaching gas concentration is kept low enough that the plasma retains its electron-Ar^+, ambipolar diffusion character along the entire length of the flow tube.

Ion–ion recombination rate constants, α, have been traditionally measured in a FALP by adding sufficient attaching gas such that an ion–ion plasma of choice is created near the reactant gas inlet port. The decay of the plasma is then monitored and fit to obtain α [19,20]. An additional gas can be added to the same inlet to convert He^+ and Ar^+ to the positive ion of inter-

[1] With a 4%/96% Ar/He buffer gas, a typical 300-K mass spectrum at the downstream end of the flow tube showed Ar^+ (97.6%, sum of 40 and 36 amu intensities), N^+ (1.1%), HeH^+ (0.6%), O^+ (0.4%), H_2O^+ (0.2%), NO^+ (<0.1%), and O_2^+ (<0.1%), so the total molecular positive ion concentration was 1%.

est. While the bulk of ion–ion recombination rate constants have been measured by this technique [20], it is limited by the electron attachment and ion–molecule chemistry occurring when large quantities of gases are added, because one must end up with a single negative ion and a single positive ion traveling together over most the length of the flow tube. In many cases, it is possible to produce only a mixture of positive ion types or negative ion types, or both [20].

Here, we present a technique to extend the ability to study ion–ion recombination in the FALP to additional species. Relative negative ion concentrations are measured as a function of the initial electron density, keeping all other conditions fixed. The initial electron concentration can be varied by changing the position of the microwave discharge, or the fraction of the He flow entering upstream of the microwave discharge (the rest entering downstream with the Ar), and to a small extent, the microwave discharge power.

After the ambipolar diffusion rate is measured, a low flow of attaching gas is introduced at a fixed point 46.5 cm from the sampling orifice of the mass spectrometer. For the cases studied in the present work, electron attachment is much faster than reaction of Ar^+ with the reactant gas, so that the positive ion composition is essentially unchanged, i.e. it remains near 98% Ar^+. If the attaching gas forms two or more anions, changes in the relative negative ion composition with plasma density will be observed if the rate constants for recombination of the various negative ions with Ar^+ differ. At low initial plasma density, little recombination will occur along the length of the flow tube, while at high concentrations, recombination will be rapid, since recombination depends on the square of the plasma density. An important aspect of the present measurements is that accurate branching fractions must be measured. This has been accomplished by operating the mass spectrometer at low resolution (typically $\Delta m = 8$ amu), high transmission energy (~8 eV), and by interfacing the mass spectrometer output to a Handyscope digital storage oscilloscope and averaging (flat-top) mass peak heights over typically one hundred mass scans for each datum to be shown below. In this manner, the branching fractions are believed precise to approximately 0.002. The accuracy will depend on any remaining mass discrimination engendered by the ion sampling system, which is mainly a concern if two ions differ considerably in mass. The potential applied to the sampling aperture (typically 0.6 V for negative ions) was set to maximize the ion signal through the mass spectrometer. Tests have been carried out for sampling aperture potentials between −0.4 and 6 V, comparing Cl^- and SF_5^- intensities. For low potentials (0–1 V), the relative intensities (e.g. the branching fractions) were constant within ±0.01. [For potentials >1 V, the signal strengths fell off, and there was evidence of discrimination against the lighter ion (a lensing effect), by as much as 0.08 in the branching fraction.]

Fig. 2 shows an example when a small concentration of $C_2Br_2O_2$ (oxalyl bromide) is added to the inlet (9.4×10^8 cm^{-3} in that case). This neutral attaches electrons rapidly to form both Br^- and Br_2^- [26]. (The oxalyl bromide data were obtained before installing a signal-averaging system, and thus show less precision than is now possible.) At low initial electron concentration, i.e. below a few times 10^9 cm^{-3}, approximately 55% of the anions are Br^- and the remaining ones Br_2^-. If there were no recombination events with Ar^+ ions, i.e. only binary electron attachment and ambipolar diffusion, then a branching fraction plot such as Fig. 2 would show two flat lines. As the initial electron density increases, the fraction of Br^- increases such that it nears 100% when the initial plasma concentration approaches 4×10^{10} cm^{-3}, because Ar^+ recombines negligibly with Br^- but significantly with Br_2^-. Measurements of electron attachment rate constants for oxalyl bromide ($(1.3 \pm 0.4) \times 10^{-7}$ cm^3 s^{-1} at 300 K) and oxalyl chloride ($(1.8 \pm 0.5) \times 10^{-8}$ cm^3 s^{-1} at 300 K) were reported earlier [26].

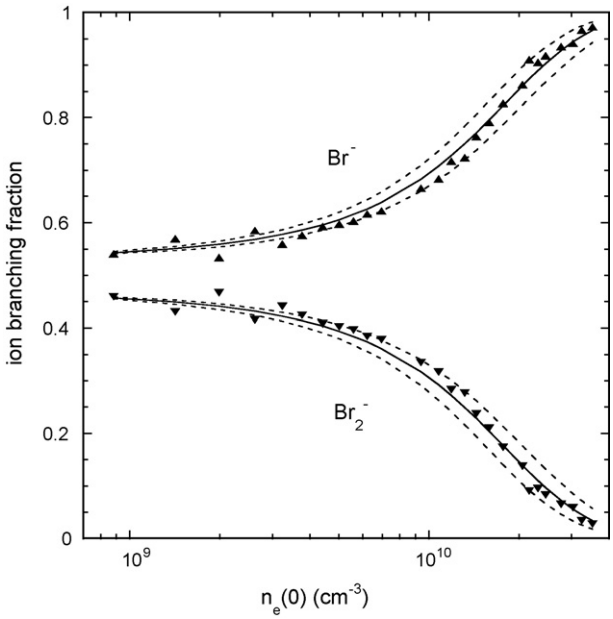

Fig. 2. Branching fractions for electron attachment to oxalyl bromide (9.42×10^8 cm^{-3}) in He buffer gas (with 4% Ar, totaling 3.22×10^{16} cm^{-3}) at 302 K, followed by Ar^+ recombination with Br_2^-. Solid curves are the best fit from numerical solution of Eqs. (2)–(7). Dashed curves utilize a recombination rate constant ±20% different from optimum.

Rate constants for the recombination rate for Ar^+ recombining with Br_2^- can be derived by modeling the kinetics in the flow tube. At present, a one-dimensional model is used. The model includes the ambipolar diffusion frequency, the electron attachment rate constant, the attachment ion product distributions, and the recombination rates for the various ions. Absolute rate constants can only be obtained with the new technique if the positive ion and one of the negative ions are monatomic so that the recombination rate between those species is negligible. The rate equations include recombination with molecular impurities (positive ions, ~1% (see footnote 1)) and with the few positive ions produced in reaction between Ar^+ and the reactant gas. These positive ions, being molecular, are assumed to recombine equally with all negative ions and do not end up affecting the results noticeably, under the conditions of the present work (low impurity level, low reactant concentration). The rate equations used for the modeling, shown for the oxalyl bromide case in which electron attachment yields Br^- (concentration n_1) and Br_2^- (concentration n_2), with corresponding branching fractions

f_1 and f_2, are:

$$\frac{dA}{dt} = -\nu_D A - kAn_r - \alpha_1 n_1 A - \alpha_2 n_2 A \quad (2)$$

$$\frac{dM}{dt} = -\nu_D M + kAn_r - \alpha_M M n_1 - \alpha_M M n_2 \quad (3)$$

$$\frac{dn_1}{dt} = k_a f_1 n_r n_e - \alpha_1 n_1 A - \alpha_M M n_1 \quad (4)$$

$$\frac{dn_2}{dt} = k_a f_2 n_r n_e - \alpha_2 n2A - \alpha_M M n_2 \quad (5)$$

$$\frac{dn_r}{dt} = -k_a n_r n_e - kAn_r \quad (6)$$

$$\frac{dn_e}{dt} = \frac{dA}{dt} + \frac{dM}{dt} - \frac{dn_1}{dt} - \frac{dn_2}{dt} \quad (7)$$

where A, n_r, and n_e represent the Ar^+, neutral reactant (oxalyl bromide in this case), and electron concentrations, respectively, and M denotes the molecular positive ion concentration, initially due to impurities in the buffer gas (~1% of A), and as a result of Ar^+ reaction with the oxalyl bromide. The electron/ion ambipolar diffusion frequency is ν_D. The reaction rate constants are k (for Ar^+ + oxalyl bromide yielding M^+), α_1 and α_2 (Ar^+ recombination with Br^- and $Br_2{}^-$), α_M (recombination between M^+ and Br^- and $Br_2{}^-$), k_a (electron attachment to the neutral reactant, measured in earlier experiments). Equation (7) expresses plasma neutrality. Note that negative ions are trapped in the space charge field of the plasma and do not diffuse, as long as the plasma density is large enough that the Debye length is less than the characteristic dimension of the apparatus, i.e. the plasma is not in the free diffusion regime. This matter has been discussed at length in earlier papers, in which similar modeling was explained in connection with thermal electron detachment reactions [35,46]. We also note that experimentally ν_D is found to increase somewhat as the initial plasma density increases, and this effect is included in Eqs. (2) and (3).

The inputs to the model are all fixed except the recombination rates, though recombination between Ar^+ and any atomic anion is estimated at 5×10^{-10} cm^3 s^{-1}, consistent with available experiment and theory. (Doubling this figure only effects the rate constant for $Ar^+ + Br_2{}^-$ by 1%. Any value smaller than 1×10^{-9} cm^3 s^{-1} for $Ar^+ + Cl^-$ or $Ar^+ + Br^-$ is essentially equivalent to zero, i.e. the experiment cannot separate such a low rate constant from the diffusive background.) The recombination rates are varied until the best fit is obtained. Within experimental uncertainties, the $Ar^+ + Br_2{}^-$ data are reproduced with a recombination rate of 3.9×10^{-8} cm^3 s^{-1}. To show the sensitivity of the fits, curves with the recombination rate 20% higher and lower than the present value are shown as dashed lines in Fig. 2. From this type of analysis, we estimate that the absolute recombination rate constants derived in this manner are accurate to 30%. The model is rather insensitive to changes in the M fraction (~1%) and to adjustment of the electron attachment rate constant, because these changes affect both negative ion types fairly equally. On the other hand, if an artificial 25% mass discrimination error is introduced into the data of Fig. 2, the recombination fit is not as good, and the value of $\alpha(Br_2{}^-)$ changes by 50%. So, accurate branching fractions are required.

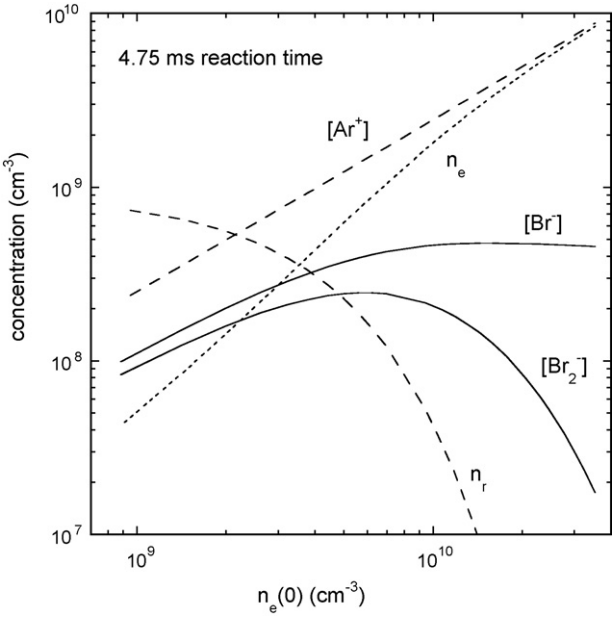

Fig. 3. Modeled concentrations of species in the plasma after 4.75-ms reaction time. The input parameters are those given in the caption to Fig. 2, along with rate constants for Ar^+ recombination with Br^- (5×10^{-10} cm^3 s^{-1}) and $Br_2{}^-$ (3.9×10^{-8} cm^3 s^{-1}) and ambipolar diffusion ($\nu_D \approx 300$ s^{-1}).

Fig. 3 shows the modeled Ar^+, n_r, n_e, Br^-, and $Br_2{}^-$ concentrations at the end of the flow tube, for the fit to the data shown in Fig. 2. In Fig. 3, the Ar^+ concentration is large enough that it is little affected by recombination with Br^- and $Br_2{}^-$, so the level of the Ar^+ line, compared to $n_e(0)$, essentially represents the loss in plasma density due to ambipolar diffusion over the 4.75-ms reaction time. The molecular positive ion concentration remains at a level of about 1% of the Ar^+ concentration, and is not shown in Fig. 3, to avoid cluttering the graph. The sum of the electron, Br^-, and $Br_2{}^-$ concentrations equals the positive ion concentration (99% Ar^+).

If there is no atomic negative ion formed in the attachment process, *relative* recombination rates can be derived with high precision since the product distributions are sensitive to the different recombination rate constants. In favorable circumstances, 5% (or possibly better) differences in relative recombination rate constants should be discernable. Even relative results would be valuable tests for theory, e.g. in providing tests of Eq. (1).

Experimental parameters implicit in the rate equations are the temperature, pressure, ion velocity, and attachment kinetics. Temperature in the AFRL FALP can be varied from 300–670 K. The temperature variability is obtained by heating the flow tube in three zones. Temperature is measured by resistance-temperature-devices (RTDs) inserted on the inside of the flow tube walls. Pressure is measured by a capacitance manometer. The plasma velocity (typically 100 m s^{-1}) is measured with the movable Langmuir probe, timing the propagation of a small pulsed disturbance in the microwave discharge [47]. All of these parameters can be measured within a few percent. All of the data reported here were obtained at 133 Pa buffer gas pressure.

3. Results

The data in Fig. 2 are best described by an $Ar^+ + Br_2^-$ recombination rate constant of $3.9 \pm 1.2 \times 10^{-8}$ cm^3 s^{-1}, at 302 K, following electron attachment to oxalyl bromide. This depends on the almost certain assumption that the $Ar^+ + Br^-$ recombination is negligible.

The next system studied involves ions generated by electron attachment to oxalyl chloride, $C_2Cl_2O_2$. Three negative ions are formed in this reaction, namely, Cl^-, Cl_2^- and the phosgene negative ion, CCl_2O^- [26]. Data obtained at 300 K are shown in Fig. 4. At low initial plasma density, the main product ion is Cl_2^- at about 65%. The remaining ions are almost equally divided between Cl^- and CCl_2O^-. As with the oxalyl bromide system, the concentrations remain approximately constant with initial plasma density until it exceeds $\sim 3 \times 10^9$ cm^{-3}. Beyond that point, both the Cl_2^- and CCl_2O^- fractions decrease and the Cl^- fraction increases. The modeling assumes a rate constant of 5×10^{-10} cm^3 s^{-1} for $Ar^+ + Cl^-$ and the rate constants for the two larger negative ions are determined from fits to numerical solutions of the rate equations, Eqs. (2)–(7), transparently extended with an additional rate equation for the third negative ion type, n_3. The best fit is obtained with rate constants of $(5.3 \pm 1.6) \times 10^{-8}$ cm^3 s^{-1} and $(8.9 \pm 2.7) \times 10^{-8}$ cm^3 s^{-1} for Ar^+ recombining with Cl_2^- and CCl_2O^-, respectively. While the absolute uncertainties indicate that these values could be similar, relative uncertainties are much tighter than those quoted above. We estimate $\alpha(Cl_2^-)/\alpha(CCl_2O^-)$ should be 1.68 ± 0.11. This plainly precludes the rates being the same.

The final system presented here stems from electron attachment to SF_6. Electron attachment to SF_6 produces mainly SF_6^-, but at higher temperatures appreciable amounts of SF_5^- are also produced. We have obtained ion–ion recombination data at 550 K, where the SF_5^- branching fraction is about 0.1. These data are shown in Fig. 5, and, like the data in Fig. 2, were obtained prior to use of a signal-averaging instrument. The SF_6^- branching fraction turns down slightly at high $n_e(0)$, while that for SF_5^- turns upward, implying that the recombination rate with Ar^+ is greater for SF_6^- (greater loss rate) than for SF_5^-. In this case only the relative recombination rate constants may be obtained. The ratio of $\alpha(SF_6^-)/\alpha(SF_5^-)$ determined from these data depends somewhat on the choice made for either $\alpha(SF_6^-)$ or $\alpha(SF_5^-)$. Other data obtained with an atomic negative ion present (described in the next paragraph) give an average value $\alpha(SF_6^-) = 4.7 \times 10^{-8}$ cm^3 s^{-1} (at 530 K). Note that the value at 530 K should be lower than that at 300 K by a factor of 0.75, according to Eq. (1). Using this value with the data shown in Fig. 5, $\alpha(SF_6^-) = 3.9 \times 10^{-8}$ cm^3 s^{-1}, and $\alpha(SF_6^-)/\alpha(SF_5^-) = 1.2$ (at 550 K), with an uncertainty of +0.3 and −0.1, for recombination with Ar^+. Application of Eq. (1) in this case is interesting, because the electron affinities of SF_6 and SF_5 differ by so much (that of SF_6 being 1.05 eV [25] and that of SF_5 being 4.2 eV [48]). Equation (1) yields 6.5×10^{-8} cm^3 s^{-1} for $Ar^+ + SF_6^-$ and 4.7×10^{-8} cm^3 s^{-1} for $Ar^+ + SF_5^-$ at 550 K, for a ratio of 1.37. The lower experimental value implies that the dependence of α on E_{be} should be weaker than given in Eq. (1), but this conclusion is not definite. If $\alpha(SF_6^-)$ were to be lower, namely, 2.74×10^{-8} cm^3 s^{-1}, then the data shown in Fig. 5 would give exactly the ratio $\alpha(SF_6^-)/\alpha(SF_5^-)$ predicted by Eq. (1). A better absolute value for $\alpha(SF_6^-)$ or $\alpha(SF_5^-)$ is required.

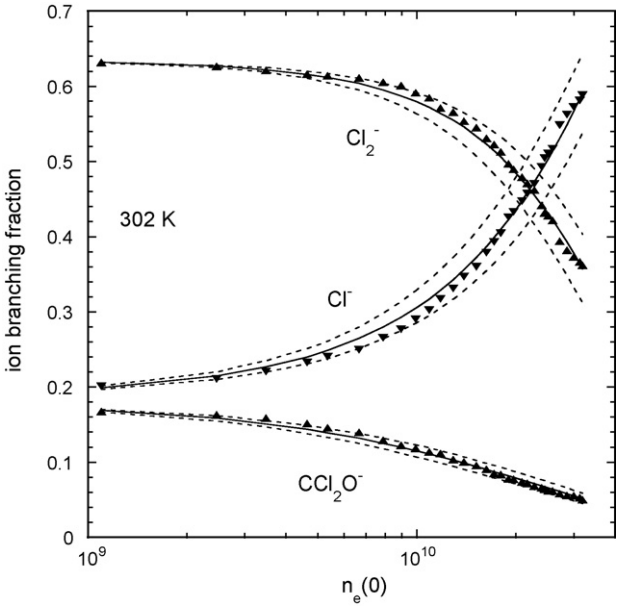

Fig. 4. Branching fractions for electron attachment to oxalyl chloride (3.71×10^9 cm^{-3}) in He buffer gas (with 4% Ar, totaling 3.22×10^{16} cm^{-3}), followed by Ar^+ recombination with Cl_2^- and CCl_2O^-. Solid and dashed lines as in Fig. 2.

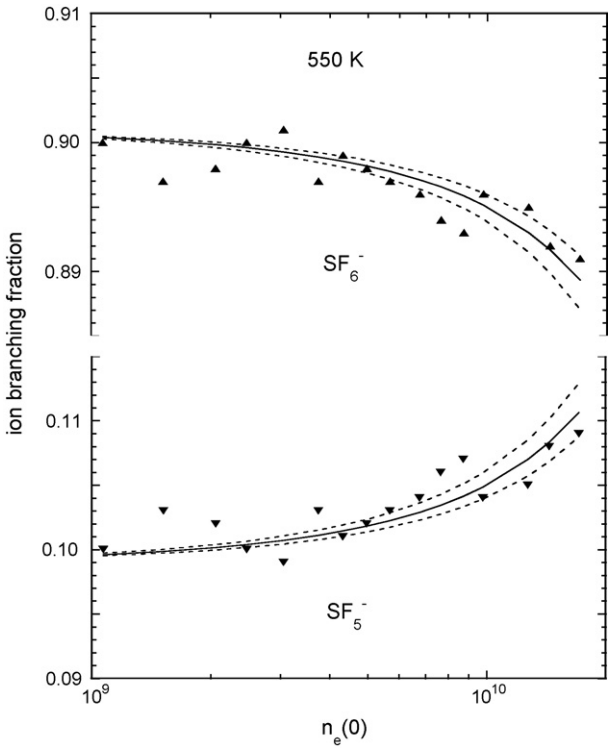

Fig. 5. Branching fractions for electron attachment to SF_6 (1.24×10^9 cm^{-3}) in He buffer gas (with 3% Ar, at 550 K, totaling 1.75×10^{16} cm^{-3}), followed by Ar^+ recombination with SF_6^- and SF_5^-. Solid and dashed lines as in Fig. 2.

Table 1
Rate coefficients for Ar^+ recombination with various negative ions measured in the present study

Ion	Temperature (K)	Rate constant ($cm^3\ s^{-1}$)	Semiempical, Eq. (1)[a] ($cm^3\ s^{-1}$)
Br_2^-	302	$(3.9 \pm 1.2) \times 10^{-8}$	Not applicable
Cl_2^-	302	$(5.3 \pm 1.6) \times 10^{-8}$	Not applicable
CCl_2O^-	302	$(8.9 \pm 2.7) \times 10^{-8}$	9.0×10^{-8}
CCl_2O^-/Cl_2^-	302	1.68 ± 0.11 ratio	Not applicable
SF_6^-/SF_5^-	550	1.2 (+0.3, −0.1) ratio	1.37[b]

[a] Eq (1) is not expected to be applicable to Br_2^- and Cl_2^- (see text); it predicts a value 1.5 times the measured rate constant.
[b] Eq (1) predicts $\alpha(SF_6^-) = 6.5$ and $\alpha(SF_5^-) = 4.7 \times 10^{-8}\ cm^3\ s^{-1}$ at 550 K.

We have attempted to introduce an atomic negative ion into the SF_6^-/SF_5^- milieu in order to put the SF_6^- and SF_5^- rate constants on an absolute scale. We did this first by mixing in a small amount of CCl_4, then by mixing in a small amount of CF_3Br. It turned out that the modeling is more complicated than first envisioned, because, in the CF_3Br case that reactant is consumed at a slower rate than is the SF_6, and the situation is reversed for CCl_4. This adds additional parameters to the modeling, with concomitant uncertainty. A second problem is that unexpected negative ions are produced at high plasma density. For example, SF_4^- ions appear in the mass spectrum at high plasma density in the SF_6 experiments, and $PSCl^-$ ions appear in preliminary work on ion–ion recombination between Ar^+ with $PSCl_2^-$ formed from $PSCl_3$. Neither of the SF_4^- nor $PSCl^-$ ions are products of electron attachment to SF_6 or $PSCl_3$ [36,51]. There is some evidence that the unexpected ions are the result of dissociation in the recombination process, followed by electron attachment to the recombination products. These few-percent unexpected ions have been ignored in plotting the SF_6 branching fractions in Figs. 5 and 6. An example is given in Fig. 6, for the case where SF_6 and CCl_4 were added to the flow tube. The resulting rate constants are $\alpha(SF_6^-) = 6.6 \times 10^{-8}\ cm^3\ s^{-1}$ and $\alpha(SF_5^-) = 4.6 \times 10^{-8}\ cm^3\ s^{-1}$ at 530 K, and a ratio $\alpha(SF_6^-)/\alpha(SF_5^-) = 1.4$, all of these numbers having considerable uncertainty. Similar data obtained with SF_6 and CF_3Br yielded rate constants 65% lower, with even greater uncertainty, because of the difficulty in determining unique recombination rate constants in the face of the large difference in the electron attachment rate constants for SF_6 ($2.2 \times 10^{-7}\ cm^3\ s^{-1}$ at 500 K) [49] and CF_3Br (estimated at $6.5 \times 10^{-8}\ cm^3\ s^{-1}$ at 530 K, from data given in Ref. [5]). The electron attachment rate constant for CCl_4 at 530 K is $3.6 \times 10^{-7}\ cm^3\ s^{-1}$ [50].

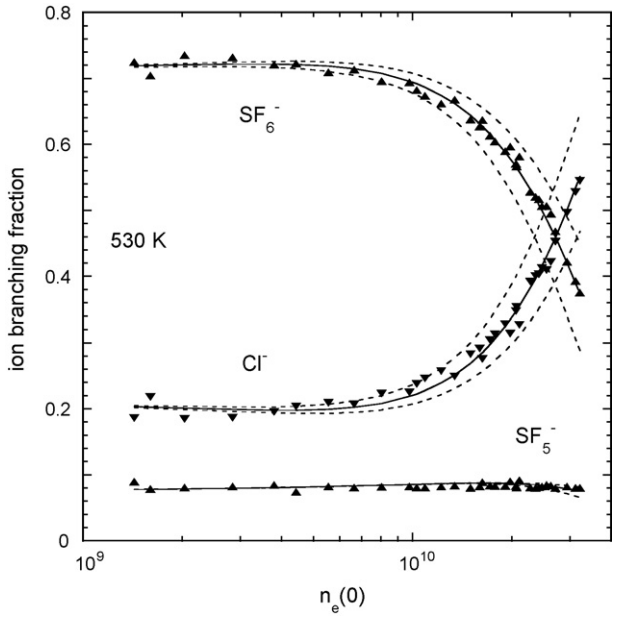

Fig. 6. Branching fractions for electron attachment to SF_6 ($2.06 \times 10^8\ cm^{-3}$) and CCl_4 ($3.35 \times 10^7\ cm^{-3}$) in He buffer gas (with 4.8% Ar, at 530 K, totaling $1.82 \times 10^{16}\ cm^{-3}$), followed by Ar^+ recombination with SF_6^- and SF_5^-. An SF_4^- ion signal is ignored for this plot because its synthesis is unclear. The SF_4^- signal reached 5% at the highest $n_e(0)$. Solid and dashed lines as in Fig. 2.

Table 1 lists all the present results. To date, most systems with four or more atoms have been found to recombine at approximately the same rate [20]. A nominal room temperature rate constant of approximately $6 \times 10^{-8}\ cm^3\ s^{-1}$ is often quoted [20,52]. Even though the upper limits for the $Ar^+ + Cl_2^-$ and $Ar^+ + Br_2^-$ rate constants are approximately equal to the nominal value, the relative rate measurements clearly show that they are smaller than for the polyatomic system $Ar^+ + CCl_2O^-$. A lower rate constant has previously been observed for triatomic systems, in the recombination of NO^+ with Cl^- and I^- [52] and for $Cl_2^+ + Cl^-$ [28]. For those systems, values of 2, 2, and $5 \times 10^{-8}\ cm^3\ s^{-1}$ were found, respectively. Presumably this stems from a lower density of states in the curve crossing region involved in the neutralization, especially for the NO^+ case. Indeed, Španěl and Smith concluded that there were no favorable curve crossings, and that the optical emissions they observed from NO must result from electron transfer on the repulsive wall of the system, which also explains the low rate constants for recombination.

For the present $Ar^+ + Cl_2^-$ case, Olson noted only one favorable curve crossing at about 7.8 Å, a result attributed to the large electron affinity of Cl_2 (2.38 eV [53]) and resulting lower reaction exothermicity rather than to its diatomic simplicity [26]. The $Ar^+ + Br_2^-$ case is similar (electron affinity of Br_2 = 2.51 eV [53]).

4. Conclusions

The present paper details a new approach to the use of the FALP technique for studies of ion–ion recombination, which allows determination of recombination rate constants when several negative ion types are present in the flow tube at once. If one

of the negative ion types is atomic, then absolute recombination rate constants may be determined, because the Ar^+ reaction with the atomic negative ion is effectively nil, providing a baseline for rate constant measurements for the other negative ions. If not, then relative rate constants are obtained for the negative ions present. The method does not depend on using the Langmuir probe to make measurements of ion concentrations, thus avoiding the problem of ion collisions with buffer gas in the plasma sheath around the probe [39–42]. The limitations of the method are:

(1) At present, the method has only been used to study recombination between negative ions and Ar^+ (clearly, Kr or Xe could replace the Ar). It is possible to add a gas such as NO, to make NO^+ (as done in [52]), provided that that gas does not react with the negative ions of interest. If the positive ion is molecular, then only relative rate constant may be determined for the various negative ions present, but accurately so.
(2) In much of the modeling done thus far, using the one-dimensional rate equations in Eqs. (2)–(7), it is difficult to fit both the low $n_e(0)$ and high $n_e(0)$ portions of the data without deviating at intermediate values of $n_e(0)$, implying a defect in the model. Whether this is due to the one-dimensional nature of the model, or to some process that is omitted, e.g. related to the products of recombination, is not known at present.

We have concentrated on improving the data collection, and now plan to solve or alleviate problems noted above (in modeling and with unexpected ions at high plasma density), and to obtain additional data and explore extensions of the method, with an eye toward measurements accurate enough to test Eq. (1). Specifically, we plan to:

(1) obtain data for additional gases which yield both atomic and molecular negative ion products upon electron attachment, notably $PSCl_3$ (57% $PSCl_2^-$ and 43% Cl^- at 298 K [51]);
(2) measure the temperature dependence of the recombination rate constants for straightforward cases such as with oxalyl chloride, oxalyl bromide, and $PSCl_3$, to test the $T^{-0.5}$ dependence in Eq. (1);
(3) measure absolute values for $\alpha(SF_6^-)$ and $\alpha(SF_5^-)$ independently, at room temperature and above, using a mixture of SF_6 and CCl_3F, which have similar electron attachment rate constants, and for $\alpha(SF_5^-)$ using a mixture of SF_5Cl and CH_3CCl_3;
(4) measure relative recombination rate constants with a molecular positive ion such as NO^+.

Acknowledgements

We are grateful for the support of the Air Force Office of Scientific Research for this work. We thank R.E. Olson for commenting on the Cl_2^- reaction. T.M.M. is under contract (FA8718-04-C0006) to the Institute for Scientific Research of Boston College.

References

[1] E.W. McDaniel, Collision Phenomena in Ionized Gases, Wiley, New York, 1964.
[2] H. Hotop, M.-W. Ruf, M. Allan, I.I. Fabricant, Adv. At. Mol. Opt. Phys. 49 (2003) 85.
[3] L.G. Christophorou (Ed.), Electron-Molecule Interactions and Their Applications, vol. 1–2, Academic Press, New York, 1984.
[4] A. Chutjian, A. Garscadden, J.M. Wadhera, Phys. Rep. 264 (1996) 393.
[5] D. Smith, P. Španěl, Adv. At. Mol. Phys. 32 (1994) 307.
[6] V.G. Anicich, An Index of the Literature for Bimolecular Gas Phase Cation-Molecule Reaction Kinetics, JPL Publication 03-19, National Aeronautics and Space Administration, Jet Propulsion Laboratory, Pasadena, California, 2003.
[7] Y. Ikezoe, S. Matsuoka, M. Takebe, A.A. Viggiano, Gas Phase Ion-Molecule Reaction Rate Constants Through 1986, Maruzen, Tokyo, 1987.
[8] J.W. McGowan, J.B.A. Mitchell, in: L.G. Christophorou (Ed.), Electron-Molecule Interactions and Their Applications, vol. 2, Academic Press, New York, 1984, pp. 65–88.
[9] A.I. Florescu-Mitchell, J.B.A. Mitchell, Phys. Rep. 430 (2006) 277.
[10] M. Larsson, R. Thomas, Phys. Chem. Chem. Phys. 3 (2001) 4471.
[11] N.G. Adams, L.M. Babcock, C.D. Molek, in: M.L. Gross, R. Caprioli, P.B. Armentrout (Eds.), The Encyclopedia of Mass Spectrometry, Theory and Ion Chemistry, vol.1, Elsevier Science, Amsterdam, 2003, pp. 555–561.
[12] J.R. Peterson, W.H. Aberth, J.T. Moseley, J.R. Sheridan, Phys. Rev. A 3 (1971) 1651.
[13] J.T. Moseley, R.E. Olson, J.R. Peterson, Case Stud. At. Phys. 5 (1975) 1.
[14] L.B. Loeb, Basic Processes of Gaseous Electronics, University of California, Berkeley, 1955.
[15] J. Sayers, Proc. R. Soc. (Lond.) A169 (1938) 83.
[16] C. Greaves, J. Electron. Contr. 17 (1964) 171.
[17] G.A. Fisk, B.H. Mahan, E.K. Parks, J. Chem. Phys. 47 (1967) 2649.
[18] M.N. Hirsch, P.N. Eisner, J.A. Slevin, Phys. Rev. 178 (1969) 175; P.N. Eisner, M.N. Hirsch, Phys. Rev. Lett. 26 (1971) 874; M.N. Hirsch, P.N. Eisner, Radio Sci. 7 (1972) 125.
[19] D. Smith, M.J. Church, Int. J. Mass Spectrom. Ion Phys. 19 (1976) 185.
[20] D. Smith, N.G. Adams, in: F. Brouillard, J.W. McGowan (Eds.), Physics of Ion–Ion and Electron-Ion Collisions, Plenum, New York, 1983.
[21] R.E. Olson, J.R. Peterson, J. Moseley, J. Chem. Phys. 53 (1970) 3391.
[22] R.E. Olson, J. Chem. Phys. 56 (1972) 2979.
[23] A.P. Hickman, J. Chem. Phys. 70 (1979) 4872.
[24] T.M. Miller, J. Chem. Phys. 72 (1980) 4659.
[25] E.P. Grimsrud, S. Chowdhury, P. Kebarle, J. Chem. Phys. 83 (1985) 1059.
[26] J.M. Van Doren, K.B. Hogan, T.M. Miller, A.A. Viggiano, J. Chem. Phys. 124 (2006) 184313.
[27] R.E. Olson, Combust. Flame 30 (1977) 243.
[28] M.J. Church, D. Smith, J. Phys. D 11 (1978) 2199.
[29] R.E. Olson (private communication).
[30] T.D. Gailey, M.F.A. Harrison, J. Phys. B 3 (1970) 1098.
[31] B. Peart, M.A. Bennett, K. Dolder, J. Phys. B 18 (1985) L439.
[32] C.Y. Chow, J.M. Goodings, Int. J. Mass Spectrom. 153 (1996) 49.
[33] A.N. Hayhurst, T.M. Sugden, Trans. Farad. Soc. 63 (1967) 1375.
[34] T.M. Miller, J.F. Friedman, A.E.S. Miller, J.F. Paulson, J. Phys. Chem. 98 (1994) 6144.
[35] T.M. Miller, Adv. At. Mol. Opt. Phys. 51 (2005) 299.
[36] T.M. Miller, A.E.S. Miller, J.F. Paulson, Xifan Liu, J. Chem. Phys. 100 (1994) 8841.
[37] P. Španěl, Int. J. Mass Spectrom. 149–150 (1995) 299.
[38] H.M. Mott-Smith, I. Langmuir, Phys. Rev. 28 (1926) 727.
[39] D. Smith, I.C. Plumb, J. Phys. D 6 (1973) 196.
[40] R. Johnsen, E.V. Shun'ko, T. Gougousi, M.F. Golde, Phys. Rev. E 50 (1994) 3994.
[41] P. Španěl, D. Smith, O. Chudacek, P. Kudrna, M. Tichy, Contrib. Plasma Phys. 35 (1995) 3.
[42] D. Trunec, P. Španěl, D. Smith, Contrib. Plasma Phys. 35 (1995) 203.
[43] F.J. Mehr, M.A. Biondi, Phys. Rev. 181 (1969) 264.
[44] M.R. Flannery, Adv. At. Mol. Opt. Phys. 32 (1994) 117.

[45] P. Španěl, L. Dittrichova, D. Smith, Int. J. Mass Spectrom. Ion Process. 129 (1993) 183.
[46] T.M. Miller, R.A. Morris, A.E.S. Miller, A.A. Viggiano, J.F. Paulson, Int. J. Mass Spectrom. Ion Process. 135 (1994) 195.
[47] As is well known, the plasma velocity exceeds the bulk He gas flow velocity. Plasma diffusion to the walls of the flow tube results in the plasma residing more toward the axis, where the peak of the parabolic radial velocity distribution of the buffer gas occurs. See E.E. Ferguson, F.C. Fehsenfeld, A.L. Schmeltekopf, Adv. At. Mol. Phys. 5 (1969) 1;
The peak of a parabolic laminar flow velocity distribution is two times the average (or bulk) He flow speed. In the present experiments, the plasma velocity, measured on axis, is 1.7 times the bulk He flow speed implying that random walk in the plasma is rapid enough that the electrons are averaged over all parts of the parabolic velocity distribution. (For the data of Fig. 2, the plasma velocity was measured along the axis to be 98 m s^{-1}, and the bulk He speed was 56.5 m s^{-1}.) In an earlier FALP experiment, the plasma velocity was measured with radially-movable probes and found to be independent of radial position, showing directly that radial diffusion averaged the plasma velocity across a diameter of the flow tube. See N.G. Adams, M.J. Church, D. Smith, J. Phys. D 8 (1975) 1409.
[48] T.M. Miller, S.T. Arnold, A.A. Viggiano, Int. J. Mass Spectrom. 227 (2003) 413.
[49] R.W. Crompton, G.N. Haddad, Aust. J. Phys. 36 (1983) 15;
Z.L. Petrović, R.W. Crompton, J. Phys. B 17 (1985) 2777.
[50] D. Smith, N.G. Adams, E. Alge, J. Phys. B 17 (1984) 461.
[51] W.B. Knighton, T.M. Miller, E.P. Grimsrud, A.A. Viggiano, J. Chem. Phys. 120 (2004) 211, We neglected to state in that paper that the experimental uncertainty in k_a was ±25%.
[52] P. Španěl, D. Smith, Chem. Phys. Lett. 258 (1996) 477.
[53] W.A. Chupka, J. Berkowitz, D. Gutman, J. Chem. Phys. 55 (1971) 2724.